Synthesis and Structural Characterization of Zirconium Silicates

Paula Ferreira,† Artur Ferreira,† João Rocha,*,† and Maria R. Soares‡

Departamento de Química and Laboratório Central de Análises, Universidade de Aveiro, 3810-193 Aveiro, Portugal

Received September 7, 2000. Revised Manuscript Received November 6, 2000

A zirconosilicate ($Na_{0.2}K_{1.8}ZrSi_3O_9 \cdot H_2O$) analogue of the small-pore mineral kostylevite (AV-8) has been prepared via hydrothermal synthesis. The thermal transformation of microporous zirconosilicates synthetic petarasite [AV-3, $Na_5Zr_2Si_6O_{18}(Cl,OH) \cdot 2H_2O$] and synthetic umbite (AM-2, $K_2ZrSi_3O_9 \cdot H_2O$) has been studied by powder XRD, TGA, ^{29}Si, and single- and triple-quantum ^{23}Na MAS NMR. The structure of AV-8 and the structures of synthetic analogues of the dense minerals parakeldyshite ($Na_2ZrSi_2O_7$) and wadeite ($K_2ZrSi_3O_9$) obtained via calcination of AV-3 and AM-2, respectively, have been Rietveld refined and fully characterized by ^{29}Si and ^{23}Na solid-state NMR.

Introduction

Zeolites are crystalline, hydrated aluminosilicates with open three-dimensional structures built of $[SiO_4]^{4-}$ and $[AlO_4]^{5-}$ tetrahedra linked to each other by sharing all the oxygens to form regular intracrystalline cavities and channels of molecular dimensions.[1] Stable microporous materials, such as zeolites, are extremely important for applications in catalysis, adsorption, ion exchange, and separation. Through the 1990s new classes of microporous materials and channel structures involving mixed octahedral−tetrahedral framework oxides have been reported.[2] So far, most of the work has concentrated on microporous titanosilicates, the most promising material being ETS-10.[3,4] However, there is tremendous room for introducing transition metals other than titanium.

Zirconium silicates occur widely in nature and their formation under hydrothermal conditions (from ≈300 to ≈550 °C) has been given considerable attention, though mainly for the solution of general geophysical and mineralogical problems (see ref 5 and references therein). More than 20 natural and synthetic zirconium silicates are known and for about one-third of them the crystal structures have been solved. Some of the first hydrothermal syntheses of zirconium silicates have been carried out by Maurice in 1949.[6] Baussy et al. summarize the early work in this field and report the hydrothermal synthesis of (among others) analogues of the minerals catapleiite ($Na_2ZrSi_3O_9 \cdot 2H_2O$) and elpidite ($Na_2ZrSi_6O_{15} \cdot 3H_2O$) at 350−500 °C.[7] These materials have also been prepared by others.[8] Jale et al. reported the hydrothermal synthesis of a potassium analogue of mineral elpidite at a relatively low temperature (200 °C).[9]

The interesting and promising chemistry of sodium zirconium silicates is clearly illustrated in the recent work of Clearfield and co-workers.[5] These workers reported on the synthesis, characterization, and properties of three novel layered materials and five other zirconium silicates. In particular, a synthetic analogue of the mineral gaidonnayite (ideal formula $Na_2ZrSi_3O_9 \cdot 2H_2O$) has been prepared. This material has also been synthesized by Rocha and Anderson and co-workers (AV-4)[10] and by Jale et al.[9]

In this paper we wish to report further studies on the chemistry of small-pore (or channel) zirconium silicate materials. Specifically, here we study the thermal transformations of synthetic petarasite and umbite and the preparation of analogues of minerals parakeldyshite and wadeite. The hydrothermal synthesis and the structural characterization of an analogue of mineral kostylevite are also described. Petarasite (Mont St. Hilaire, Québec, Canada) is a rare mineral with the formula $Na_5Zr_2Si_6O_{18}(Cl,OH) \cdot 2H_2O$.[11] We previously reported the synthesis and characterization of AV-3, an analogue of petarasite.[10,12] Ti-AM-2 is a synthetic potassium titanium silicate analogue of the mineral umbite, found in the Khibiny alkaline massif (Russia).[13] Although the ideal formula of umbite is $K_2ZrSi_3O_9 \cdot H_2O$, a pronounced substitution of titanium for zirconium

* To whom correspondence should be addressed.
† Departamento de Química.
‡ Laboratório Central de Análises.

(1) Barrer, R. M.; *Hydrothermal Chemistry of Zeolites*, Academic Press: New York, 1974.
(2) Anderson, M. W.; Rocha, J. *Eur. J. Inorg. Chem*. **2000**, 801.
(3) Kuznicki, S. M. U.S. Patent 4,853,202, 1989. Kuznicki, S. M. U.S. Patent 4,938,989, 1990.
(4) Anderson, M. W.; Terasaki, O.; Ohsuna, T.; Phillippou, A.; Mackay, S. P.; Ferreira, A.; Rocha, J.; Lidin, S. *Nature* **1994**, *367*, 347.
(5) Bortun, A. I.; Bortun, L. N.; Clearfield, A. *Chem. Mater.* **1997**, *9*, 1854.
(6) Maurice, O. D. *Econ. Geol.* **1949**, *44*, 721.
(7) Baussy, G.; Caruba, R.; Baumer, A.; Turco, G. *Bull. Soc. Fr. Minér. Crystallogr.* **1974**, *97*, 433.
(8) Chao, G. Y.; Watkinson, D. H. *Can. Miner.* **1974**, *12*, 316.
(9) Jale, S. R.; Ojo, A.; Fitch, F. R. *Chem. Commun.* **1999**, 411.
(10) Lin, Z.; Rocha, J.; Ferreira, P.; Thursfield, A.; Agger, J. R.; Anderson, M. W. *J. Phys. Chem. B* **1999**, *103*, 957.
(11) Ghose, S.; Wan, C.; Chao, G. Y. *Can. Miner.* **1980**, *18*, 503. Chao, G. Y.; Chen, T. T.; Baker, J. *Can. Miner.* **1980**, *18*, 497.
(12) Rocha, J.; Ferreira, P.; Lin, Z.; Agger, J. R.; Anderson, M. W. *Chem. Commun.* **1998**, 1269.
(13) Ilyushin, G. D. *Inorg. Mater.* **1993**, *29*, 853.

10.1021/cm0007196 CCC: $20.00
Published on Web 01/05/2001

occurs in nature. The successful synthesis of a complete solid solution between $K_2TiSi_3O_9 \cdot H_2O$ and $K_2ZrSi_3O_9 \cdot H_2O$ has been reported.[10,14,15] Moreover, the synthesis, characterization, and ion-exchange behavior of $K_2TiSi_3O_9 \cdot H_2O$ and its protonated forms were also reported recently by Clearfield and co-workers.[16] Umbite and kostylevite[17] are the orthorhombic and monoclinic polymorphs of $K_2ZrSi_3O_9 \cdot H_2O$, respectively. These minerals exhibit the same octagonal, heptagonal, and hexagonal distorted tunnels and windows, delimited by edges from tetrahedra and octahedra alternating in exactly the same way. The difference between the two solids resides in the fact that kostylevite is a cyclohexasilicate and umbite is a long-chain polysilicate.[18] Liu et al.[19] recently reported the synthesis of UND-1, a titanosilicate analogue of kostylevite. Here, the zirconeous synthetic analogue of kostylevite is named AV-8.

The dense mineral wadeite found in the West Kimberley area, Western Australia, has the ideal formula $K_2ZrSi_3O_9$.[20] A series of compounds, $A_2BSi_3O_9$ (A = K, Rb; B = Ti, Sn), whose structures are isomorphous with the structure of wadeite was reported.[21] Parakeldyshite (ideal formula $Na_2ZrSi_2O_7$)[22] was found in nepheline syenite pegmatites in foyaite near Larvikin in southern Norway.

Experimental Section

Synthesis. The syntheses were carried out in Teflon-lined autoclaves under hydrothermal conditions. In all syntheses, the autoclaves were removed and quenched in cold water after an appropriate time. The off-white microcrystalline powders were filtered, washed at room temperature with distilled water, and dried at 100 °C. Zirconeous AM-2 and AV-3 were prepared following a previously published method.[10]

Typical AV-8 Synthesis. An alkaline solution was made by mixing 2.10 g of precipitated silica (BDH), 5.00 g of KOH (Merck), 2.00 g of NaOH (Merck), and 16.25 g of H_2O. An amount of 1.99 g of $ZrCl_4$ (Aldrich) was added to this solution and stirred thoroughly. The gel, with a composition 0.71:1.26:1.00:0.24:25.7 Na_2O:K_2O:SiO_2:ZrO_2:H_2O, was autoclaved under autogenous pressure for 5 days at 230 °C.

Characterization. Powder X-ray diffraction (XRD) data were collected on a Philips X'pert MPD diffractometer using Cu Kα radiation with a curved graphite monochromator and a proportional detector. Rietveld refinement was performed using the program FULLPROF.[23] Data were collected at room temperature between 6 and 140°, in 2θ with a step size of 0.02° and a count time of 7 s/step. Scanning electron microscopy (SEM) images were recorded on a Hitachi S-4100 microscope.

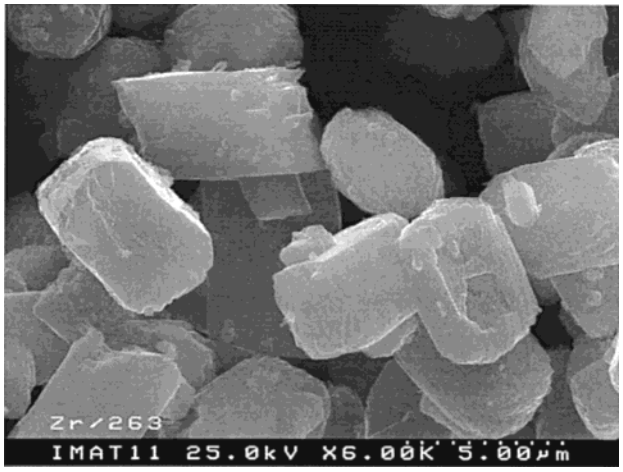

Figure 1. SEM image of synthetic kostylevite, AV-8.

^{23}Na and ^{29}Si NMR spectra were recorded at 105.85 and 79.49 MHz, respectively, on a (9.4 T) Bruker MSL 400P spectrometer. ^{29}Si magic-angle spinning (MAS) NMR spectra were recorded with 40° pulses, spinning rates of 5.0−5.5 kHz, and 35 s of recycle delay. Chemical shifts are quoted in ppm from TMS. Single-quantum ^{23}Na MAS NMR spectra were measured using short and powerful radio frequency pulses (0.6 μs, equivalent to a 15° pulse angle), a spinning rate of 15 kHz, and a recycle delay of 2 s. Chemical shifts are quoted in ppm from 1 M aqueous NaCl. The triple-quantum (3Q) ^{23}Na MAS NMR spectra [24] were recorded with radio frequency magnetic field amplitudes of ≈160 kHz; 210−256 data points were acquired in the t_1 dimension in increments of 7 μs. To produce pure absorption line shapes in the 3Q MAS spectra, the optimum conditions for excitation and transfer of the (±3Q) coherences using a simple two-pulse sequence were used. The phase cycling was composed of six phases for the selection of 3Q coherences. This phase cycling was combined with a classic overall four-phase cycle to minimize phase and amplitude missettings of the receiver. The ppm scale was referenced to υ_0 frequency in the υ_2 domain and to $3\upsilon_0$ in the υ_1 domain (reference 1 M aqueous NaCl).

The adsorption isotherms were measured on a C.I. Instruments electrobalance MK2-M5 connected to a vacuum manifold line. Each sample (≈0.1 g) was dehydrated overnight at 450 °C to an ultimate pressure of 10^{-4} mbar and then cooled to room temperature. Diffusion of water was found to be so slow in the samples studied that the adsorption data points were not true equilibrium points. Consequently, an arbitrary time of 60 min was chosen for the delay before each point was recorded. Thermogravimetric (TGA) curves were measured with a TGA-50 analyzer. The samples were heated under air at a rate of 5 °C/min. All materials were routinely characterized by differential scanning calorimetry, Fourier transform infrared, Raman, and diffuse-reflectance ultraviolet spectroscopies, but these data will not be presented here.

Results and Discussion

Characterization of AV-8 (Synthetic Zirconeous Kostylevite). SEM (Figure 1) shows that AV-8 crystals are small, parallelepiped <5 μm in length. Within experimental error, the molecular formula of AV-8 determined by EDS analysis of different crystals is $Na_{0.2}K_{1.8}ZrSi_3O_9 \cdot H_2O \cdot nH_2O$. The total AV-8 mass loss (ascertained by TGA) between 30 and 450 °C is ≈5.6%, corresponding to the loss of approximately one water molecule. This reversible water loss occurs in a single step from 90 to 425 °C and powder XRD shows that the

(14) Poojary, D. M.; Bortun, A.; Bortun, L. N.; Clearfield, A. *Inorg. Chem.* **1997**, *36*, 3072.
(15) Clearfield, A.; Bortun, A. I.; Bortun, L. N.; Poojary, D. M.; Khainakov, S. A. *J. Mol. Struct.* **1998**, *470*, 207.
(16) Bortun, A. I.; Bortun, L. N.; Poojary, D. M.; Xiang, O.; Clearfield, A. *Chem. Mater.* **2000**, *12*, 294.
(17) Ilyushin, G. D.; Khomyakov, A. P.; Shumyatskaya, N. G.; Voronkov, A. A.; Nevskii, N. N.; Iliukhin, V., V.; Belov, N. V. *Sov. Phys. Dokl.* **1981**, *26*, 118.
(18) Dadachov, M. S.; Le Bail, A. *Eur. J. Solid State Inorg. Chem.* **1997**, *34*, 381.
(19) Liu, X.; Shang, M.; Thomas, J. K. *Microporous Mater.* **1977**, *10*, 273.
(20) Henshaw, D. E. *Mineral. Mag.* **1955**, *30*, 585.
(21) Choisnet, J.; Deschanvres, A.; Raveau, B. *J. Solid State Chem.* **1973**, *7*, 408.
(22) Raade, G.; Mladek, M. H. *Can. Mineral.* **1977**, *15*, 102.
(23) Rodriguez-Carvajal, J. *FULLPROF Program for Rietveld Refinement and Pattern Matching Analysis*; Abstracts of the Satellite Meeting on Powder Diffraction of the XVth Congress of the International Union of Crystallography, Toulouse, France, 1990; p 127.
(24) Rocha, J.; Esculcas, A. P.; Fernandez, C.; Amoureux, J.-P.; *J. Phys. Chem.* **1996**, *100*, 17889.

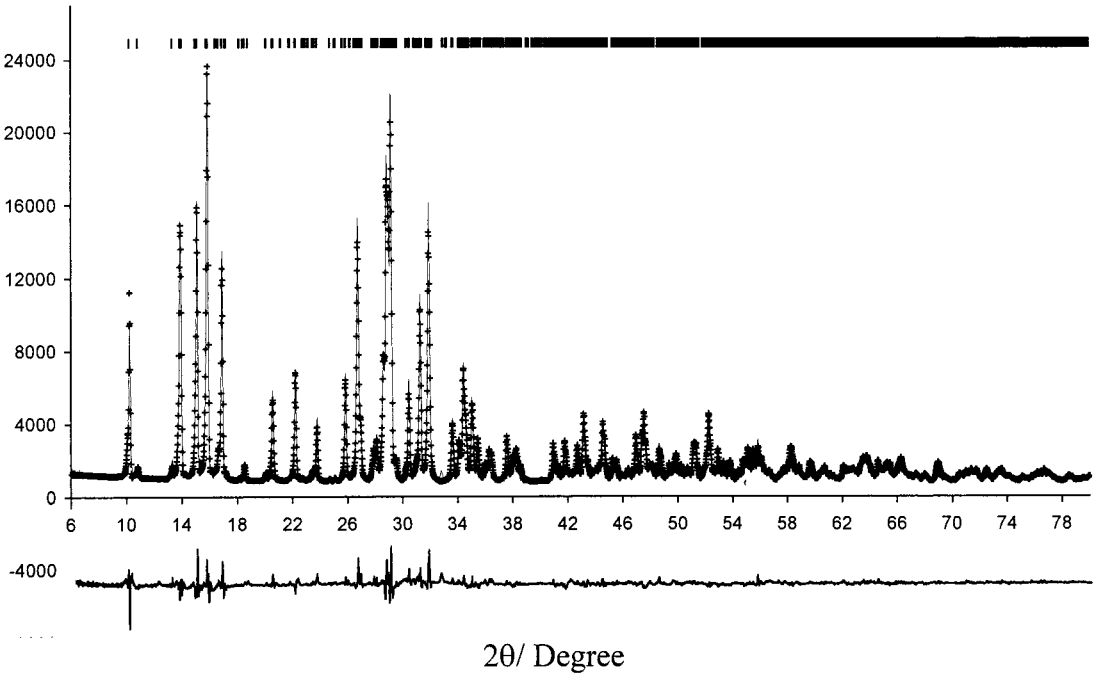

Figure 2. Observed, calculated, and difference powder XRD pattern of synthetic kostylevite, AV-8.

Table 1. Crystallographic Data for Zirconium Silicates

	AV-8	synthetic wadeite	synthetic parakeldyshite
space group	$P2_1/c$	$P63/m$	$P\bar{1}$
cell parameters:			
a (Å)	6.556 (2)	6.9291(2)	6.6364(4),
b (Å)	11.697(4)	6.9291(2)	8.8120(5),
c (Å)	13.187(4)	10.1848(4)	5.4233(3),
	$\alpha = 90.0000$	$\alpha = 90.0000$	$\alpha = 92.697(4)$
angles (°)	$\beta = 105.250(1)$	$\beta = 90.0000$	$\beta = 94.204(3)$
	$\gamma = 90.000$	$\gamma = 120.0000$	$\gamma = 71.355(3)$
V (Å^3)	981.2 (7)	423.49(3)	299.61(3)
no. of reflns/ parameters	2236/79	340/32	618/69
R_{wp}	8.46	7.95	15.7
R_p	6.00	5.45	9.66
R_F	3.25	2.39	4.47
χ^2	7.33	4.47	15.6

Table 2. Atomic Coordinates and Isotropic Thermal Parameters for AV-8

name	x	y	z	B_{iso} (Å^2)
K(1)	−0.3171(8)	0.8831(3)	0.3869(3)	2.9(1)
Na−K(2)	0.7911(2)	0.5472(4)	0.5846(4)	2.9(1)
Zr	−0.3171(8)	0.8831(3)	0.3870(3)	2.9(1)
Si(1)	−0.162(1)	0.4690(5)	0.1550(4)	1.17(7)
Si(2)	0.2143(7)	0.7387(4)	−0.0167(4)	1.17(7)
Si(3)	−0.410(9)	0.6870(5)	0.1519(4)	1.17(7)
O(1)	0.052(2)	0.5402(9)	0.1974(8)	3.2(1)
O(2)	0.080(1)	0.7628(7)	0.0596(6)	3.2(1)
O(3)	−0.192(2)	0.7480(8)	0.2035(7)	3.2(1)
O(4)	0.189(2)	0.8944(8)	0.2535(8)	3.2(1)
O(5)	0.165(2)	0.6896(9)	0.3834(8)	3.2(1)
O(6)	0.435(2)	0.6875(9)	0.2267(8)	3.2(1)
O(7)	0.149(2)	0.8946(9)	0.4470(9)	3.2(1)
O(8)	0.355(2)	1.0552(9)	0.3776(8)	3.2(1)
O(9)	0.463(2)	0.7453(8)	0.0363(9)	3.2(1)
Ow	0.607(2)	0.5052(8)	0.3850(9)	2.6(3)

framework is stable up to ≈450 °C. The study of the phases that form by thermal decomposition of AV-8 is currently in progress. The water adsorption isotherms (not shown) indicate that water diffusion in the pores of AV-8 is very slow, perhaps due to the presence of potassium ions in this small-pore system. Isotherms are of type I because of the occurrence of micropore-filling phenomena. The sorption capacity estimated at $P/P_0 = 0.4$ is ≈0.98 mmol g^{-1}. No significant nitrogen adsorption could be measured.

The observed and final Rietveld refinement profiles are shown in Figure 2, while unit cell parameters and atomic coordinates (space group $P2_1/c$) are collected in Tables 1 and 2. The sample contains a small (≈3 wt %) amount of the orthorhombic polymorph AM-2 (synthetic zirconeous umbite) and this was taken into account in the Rietveld refinement. The structure of AV-8 and kostylevite (Figure 3a) consists of six-membered rings formed by SiO_4 tetrahedra and isolated ZrO_6 octahedra. To coordinate the latter, the six-membered rings are tilted with respect to the main channel axis. Each ZrO_6 octahedron connects to six SiO_4 tetrahedra on the three six-membered rings of SiO_4 tetrahedra. In this way, three three-membered rings are formed while each SiO_4 tetrahedron connects to both two isolated ZrO_6 octahedra and two SiO_6 tetrahedra of the same six-membered ring. Then, 4-Å-diameter channels are formed along the [100] direction with eight-membered rings containing −O−Si−O−Zr−O− linkages. The wall of the channel is covered by seven-membered rings (three ZrO_6 octahedra and four SiO_4 tetrahedra), which are composed of −Si−O−Si−O− and −Zr−O−Si−O− and of the three-membered rings. There are two cation sites in the structure of AV-8. One is only occupied by K^+ and is located near the center of the seven-membered ring of the wall. In this site K^+ is coordinated by four framework oxygens from the seven-membered ring and two oxygens from adjacent six-membered rings of SiO_4 tetrahedra. The other cation site has an occupation of 80% K^+, 20% Na^+; it is located in the large channel near the wall and is coordinated by six framework oxygens of the wall and two water molecules.

The ^{29}Si MAS NMR spectrum of AV-8 (Figure 4a) displays a peak at −85.7 ppm and two overlapping peaks at −86.5 ppm in an ≈1:2 intensity ratio. This is in accord with the structure of AV-8, which calls for the

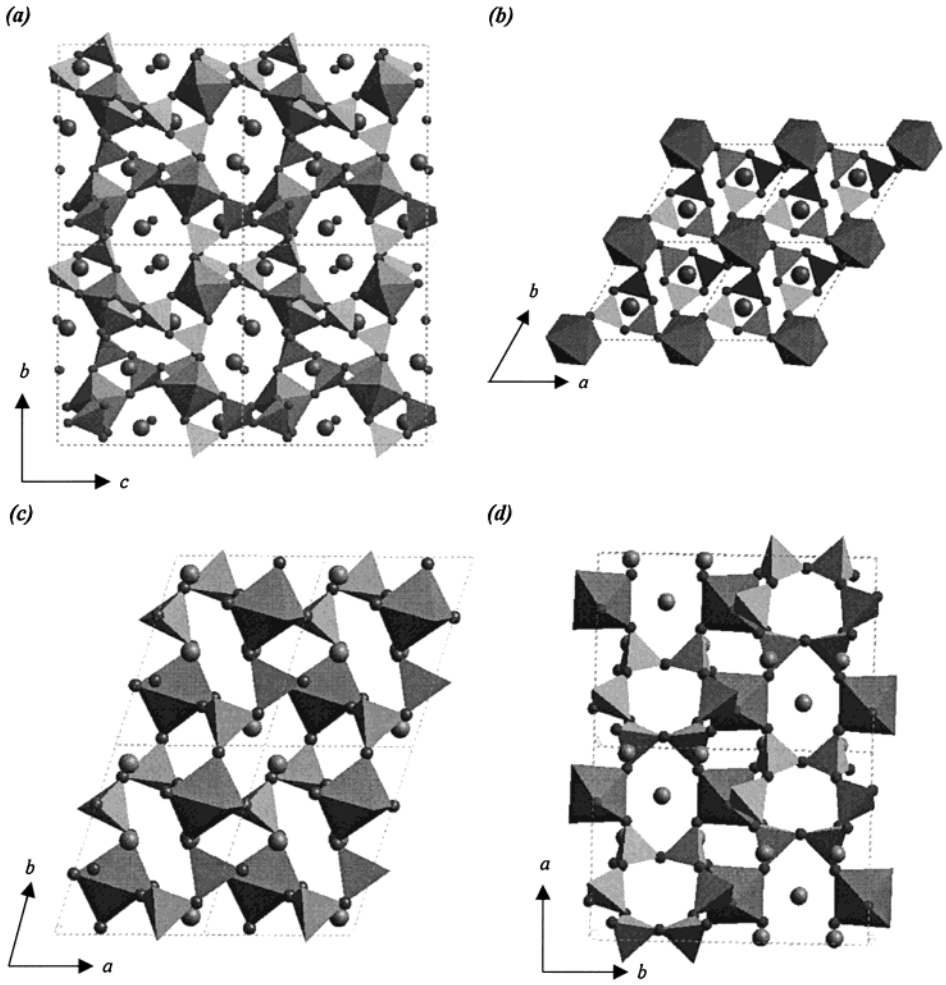

Figure 3. Polyhedral (SiO_4 tetrahedra, ZrO_6 octahedra) representation of the structures of (a) kostylevite and AV-8, (b) wadeite, (c) parakeldyshite, and (d) petarasite. Large circles depict K^+ (kostylevite and wadeite) or Na^+ ions. Small circles depict oxygen atoms.

presence of three unique Si(2Si, 2Zr) sites (silicon atoms connected to two silicon and two zirconium atoms via oxygen bridges) with equal populations. From the mean Si−O distance calculated by Rietveld refinement (Table 3) and considering the well-known correlation between the ^{29}Si NMR chemical shifts and the SiO bond length in silicates,[22] it is possible to tentatively ascribe the first peak to Si(3) and the two overlaping peaks to Si(1) and Si(2) with similar Si−O distances. For comparison, titaneous synthetic AM-2 (orthorhombic polymorph) gives three peaks at −85.9, 86.2, and −87.3 ppm while zirconeous Zr-AM-2 gives a single broad resonance at −86.5 ppm (Figure 4b). The ^{23}Na MAS NMR spectrum (not shown) contains a single peak at 1.7 ppm due to the partial occupation of the K(2) by sodium ions.

Transformation of AM-2 into Synthetic Wadeite. The transformation of synthetic umbite into wadeite was recently reported by Clearfield and co-workers.[14] TGA indicates that Zr-AM-2 reversibly loses ≈5% water in a single step from 250 to 450 °C.[10] Materials calcined at ≈450−850 °C give powder XRD patterns (Figure 5) that, although broader, are similar to the pattern of parent Zr-AM-2. At 900 °C the pattern is still essentially the same but close inspection reveals small differences. Synthetic wadeite forms between ≈950 and ≈1150 °C. At 1200 °C the material is totally amorphous. Spot EDS analyses of different crystals of the 1100 °C calcined Zr-AM-2 material shows that the Si/Zr ratio is ≈3, as in the synthetic analogues of umbite. This evidence is in good agreement with the Si/Zr ratio of 3 of the wadeite structure.

^{29}Si MAS NMR spectra of Zr-AM-2 and calcined materials are shown in Figure 6. Parent Zr-AM-2 and materials calcined up to ≈850 °C give a single broad peak at −86.5 ppm. The fwhm is 115 Hz for Zr-AM-2 and it increases to 132 Hz at 800 or 850 °C. This is in accord with the powder XRD evidence and suggests that dehydration introduces some disorder into the structure. The spectrum of the sample calcined at 900 °C displays a main peak at −86.5 ppm with shoulders at approximately −84.3, −87.1, and −88.1 ppm. A broad and faint peak is also seen at approximately −91 ppm. Thus, ^{29}Si MAS NMR suggests that the framework of Zr-AM-2 begins to collapse at ≈850 °C and its transformation into wadeite may not be direct but proceeds through an unknown intermediate. This possibility requires further investigation. At 950 °C the samples give a relatively sharp (fwhm 93 Hz) resonance at −91.4 ppm, attributed to wadeite, and faint peaks at −89.6 and −90.2 ppm. Above this temperature and up to ≈1200 °C wadeite forms; the most crystalline materials (sharper, fwhm 78 Hz, resonance) are obtained at ≈1100 °C. Samples

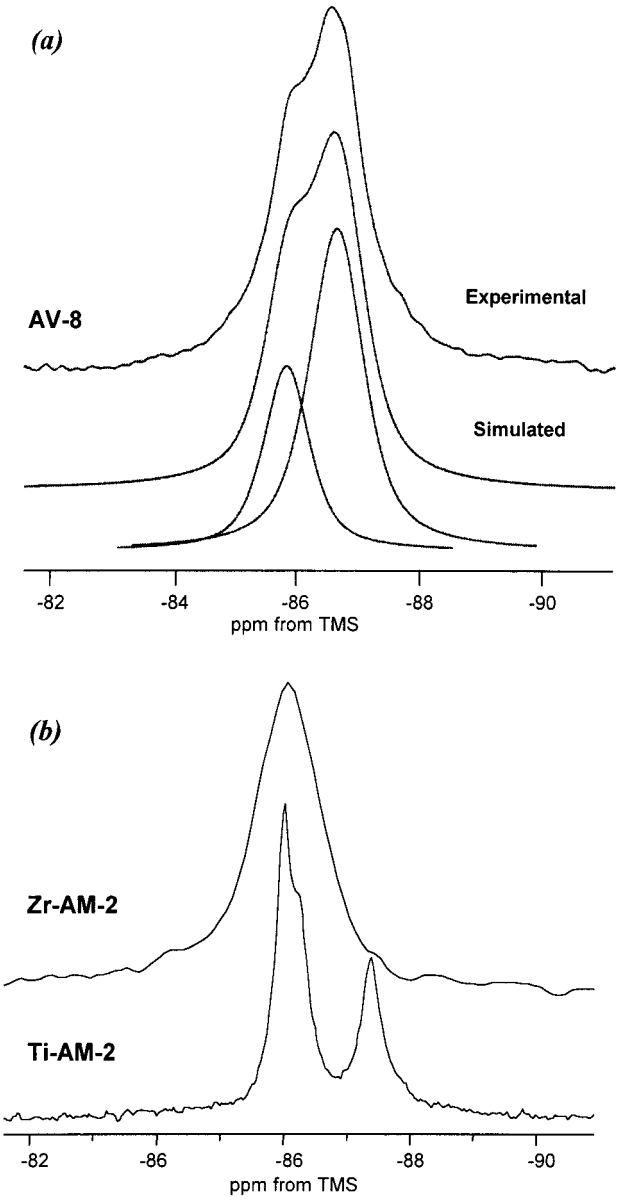

Figure 4. ^{29}Si MAS NMR spectra of (a) synthetic kostylevite, AV-8, and (b) Ti-AM-2 and Zr-AM-2.

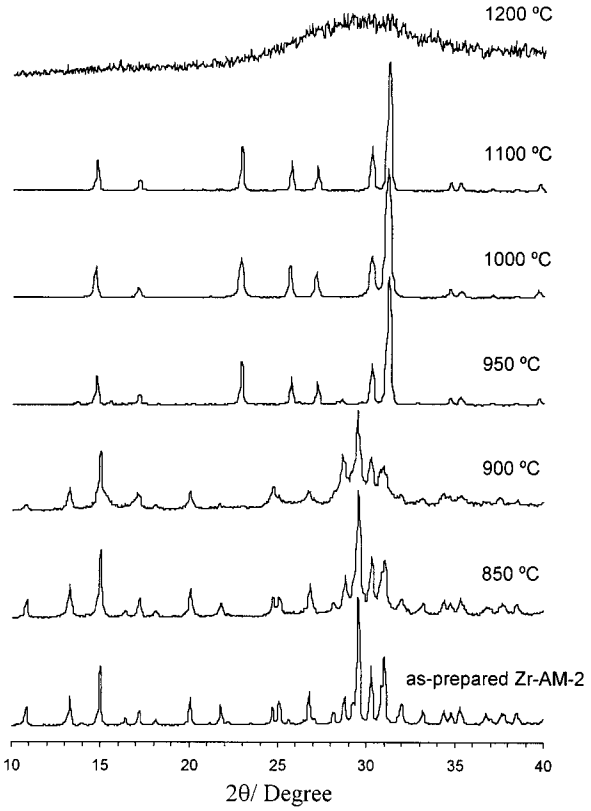

Figure 5. Powder XRD patterns of as-prepared Zr-AM-2 and materials calcined in air at the temperatures indicated for 6 h.

Table 3. Bond Distances (Å) for Zirconium Silicates

AV-8		synthetic wadeite		synthetic parakeldyshite	
Zr−O(6)	2.044	Zr−O(1)	2.087	Zr(1)−O(1)	2.082
Zr−O(3)	2.065	Zr−O(1)	2.087	Zr(1)−O(6)	2.084
Zr−O(5)	2.116	Zr−O(1)	2.087	Zr(1)−O(5)	2.086
Zr−O(1)	2.128	Zr−O(1)	2.087	Zr(1)−O(3)	2.105
Zr−O(4)	2.138	Zr−O(1)	2.087	Zr(2)−O(7)	2.133
Zr−O(2)	2.136	Zr−O(1)	2.087	Zr(2)−O(4)	2.160
Si(1)−O(4)	1.536	Si−O(1)	1.573	Si(1)−O(4)	1.552
Si(1)−O(8)	1.584	Si−O(1)	1.573	Si(1)−O(1)	1.577
Si(1)−O(1)	1.602	Si−O(2)	1.630	Si(1)−O(3)	1.582
Si(1)−O(7)	1.625	Si−O(2)	1.634	Si(1)−O(2)	1.610
Si(2)−O(2)	1.528	K−O(1)	2.841	Si(2)−O(6)	1.525
Si(2)−O(5)	1.523	K−O(1)	2.841	Si(2)−O(5)	1.621
Si(2)−O(9)	1.601	K−O(1)	2.841	Si(2)−O(7)	1.643
Si(2)−O(7)	1.654	K−O(1)	3.131	Si(2)−O(2)	1.677
Si(3)−O(3)	1.580	K−O(1)	3.131	Na(1)−O(2)	2.384
Si(3)−O(6)	1.589	K−O(1)	3.131	Na(1)−O(5)	2.446
Si(3)−O(8)	1.652	K−O(2)	3.254	Na(1)−O(4)	2.451
Si(3)−O(9)	1.677	K−O(2)	3.254	Na(1)−O(2)	2.543
K(1)−O(1)	2.944	K−O(2)	3.254	Na(1)−O(1)	2.729
K(1)−O(3)	3.171			Na(1)−O(1)	2.861
K(1)−O(4)	3.254			Na(2)−O(5)	2.449
K(1)−O(6)	3.245			Na(2)−O(7)	2.542
K(1)−O(7)	2.949			Na(2)−O(6)	2.575
K(1)−O(8)	2.922			Na(2)−O(4)	2.603
K(1)−O(8)	3.260			Na(2)−O(7)	2.630
K(1)−O(9)	3.114			Na(2)−O(4)	2.702
K(2)−O(1)	2.968			Na(2)−O(3)	2.753
K(2)−O(2)	2.972			Na(2)−O(7)	2.845
K(2)−O(3)	2.850				
K(2)−O(4)	3.031				
K(2)−O(5)	2.804				
K(2)−O(9)	3.192				
K(2)−Ow	2.637				
K(2)−Ow	2.810				

calcined at 1200 °C give a very broad ^{29}Si MAS NMR peak (not shown) centered at −90 ppm, characteristic of an amorphous material.

Tables 1 and 4 and Figure 7 give the results of the Rietveld refinement of the structure of synthetic wadeite obtained by calcining Zr-AM-2 at 1100 °C. The structure of wadeite (Figure 3b) is based on a framework of silica tetrahedra, the potassium and zirconium atoms fitting into the interstices.[14,20] The fundamental unit of these frameworks is the condensed cyclic trisilicate group. The Zr atoms are located on the origin of the crystal lattice and they form layers in the *ab* planes at $z = 0$ and $^1/_2$. Within these metal layers the Zr atoms occupy the corners of equilateral triangles and, thus, for a given Zr there are six surrounding triangles of Zr atoms in the *ab* plane. The trisilicate exists as a nonplanar cyclic group and its center is shifted halfway between the successive Zr layers along the *c* axis. The K^+ ions reside in the centers of the Zr triangles in the *ab* plane and are sandwiched between two adjacent cyclic trisilicate groups along the *c* axis. The structure of wadeite and umbite (Zr-AM-2) are different. In fact, in the latter the trisilicate group forms infinite linear chains and, thus, is not cyclic.[13] Clearfield and co-workers[14] suggested

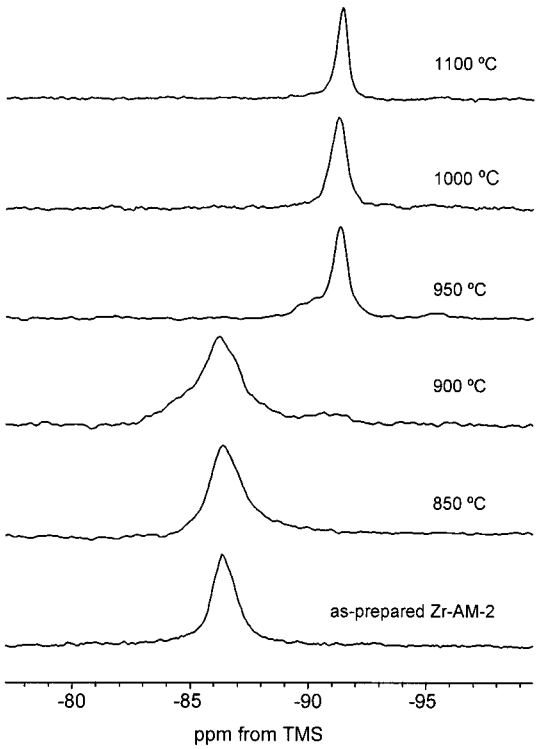

Figure 6. ^{29}Si MAS NMR of as-prepared Zr-AM-2 and materials calcined in air at the temperatures indicated for 6 h.

that umbite converts into wadeite through a lattice transformation described by a certain matrix, which converts the unit cell dimensions of the former to a lattice with parameters similar to those of wadeite. However, this matrix cannot be used to convert the atomic positions among the two phases because of the two different forms of trisilicate groups present. The Si−O distances (Table 3) in the crystal structure of wadeite are around 1.60 Å,[20] in accord with the values obtained here for the calcined materials (average Si−O distance 1.606 Å).

Table 4. Atomic Coordinates and Isotropic Thermal Parameters for Synthetic Wadeite (Zr-AM-2 Calcined at 1100 °C for 6 h)

name	*x*	*y*	*z*	B_{iso} (Å^2)
K	0.667	0.333	0.5572(1)	2.13(4)
Zr	0.000	0.000	0.000	0.97(2)
Si	0.3859(3)	0.2589(3)	0.250	0.91(4)
O(1)	0.2562(3)	0.2337(4)	0.1185(2)	1.78(6)
O(2)	0.4906(5)	0.0942(5)	0.250	1.96(9)

Transformation of AV-3 into Synthetic Parakeldyshite. TGA data on synthetic petarasite (AV-3) was reported previously.[10] The total mass loss between 30 and 800 °C is 5.3% and is due to the release of molecular water, structural and adsorbed. Between ≈800 and ≈1050 °C a second mass loss of 3.1% occurs as a result of the loss of Cl and OH.[11] Although the powder XRD patterns of AV-3 and materials calcined up to ≈800 °C (Figure 8) are similar, some differences are seen in the line width of the reflections. Parent AV-3 and a sample calcined at 750 °C and rehydrated in air overnight at room temperature display similar TGA and powder XRD patterns (not shown). The collapse of the AV-3 framework begins at ≈850 °C and at ≈1000 °C is essentially finished. Synthetic parakedyshite is the only crystalline phase present between 1000 and 1200 °C. Above the latter temperature melting occurs. The fact that the AV-3 framework does not collapse until the release of Cl indicates that this is an essential constituent of the structure.[10] Spot EDS analysis of AV-3 after calcination at different temperatures showed that the Si/Zr ratio of 3.1 for the as-synthesized AV-3 decreases to 2.2 after calcination at 1100 °C, which is in good agreement with the Si/Zr ratio of 2 in parakeldyshite. Silicon-rich particles were detected in the samples calcined at temperatures above 900 °C.

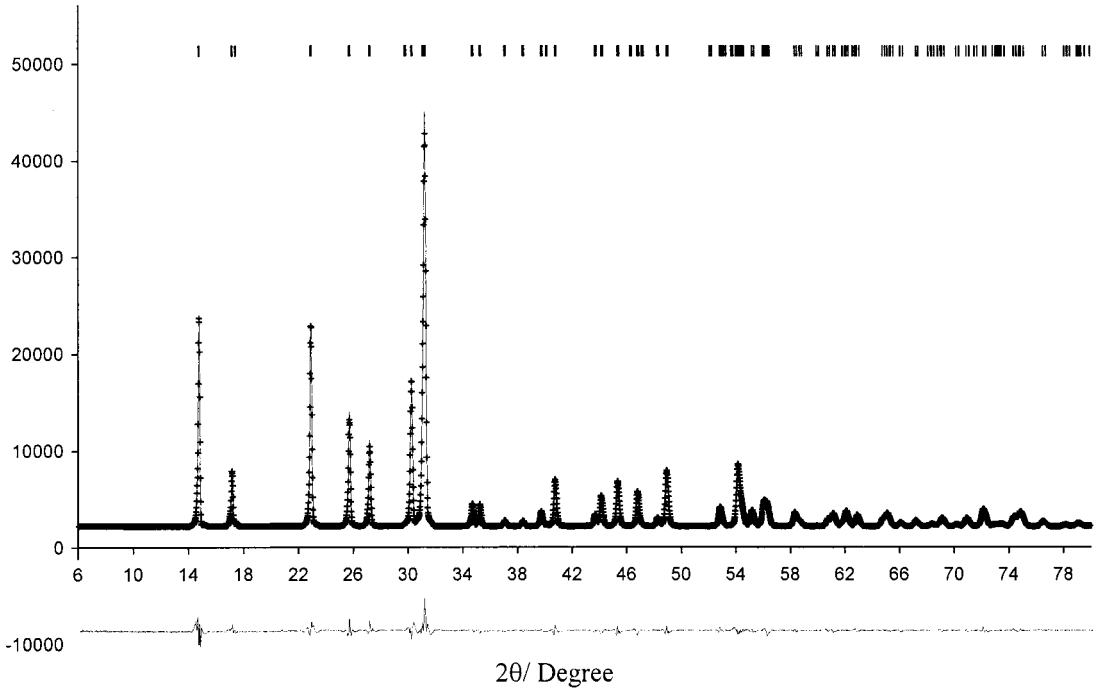

Figure 7. Observed, calculated, and difference powder XRD pattern of synthetic wadeite obtained by calcining Zr-AM-2 at 1100 °C in air for 6 h.

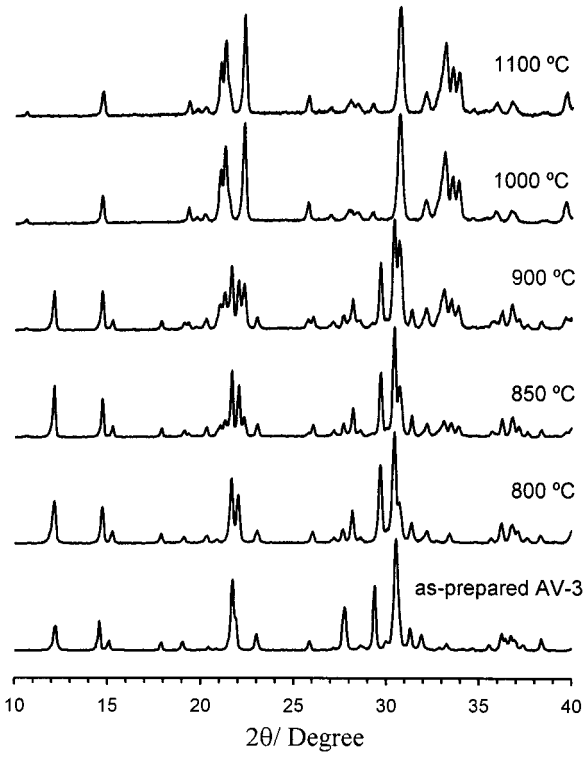

Figure 8. Powder XRD patterns of AV-3 and materials calcined in air at the temperatures indicated for 6 h.

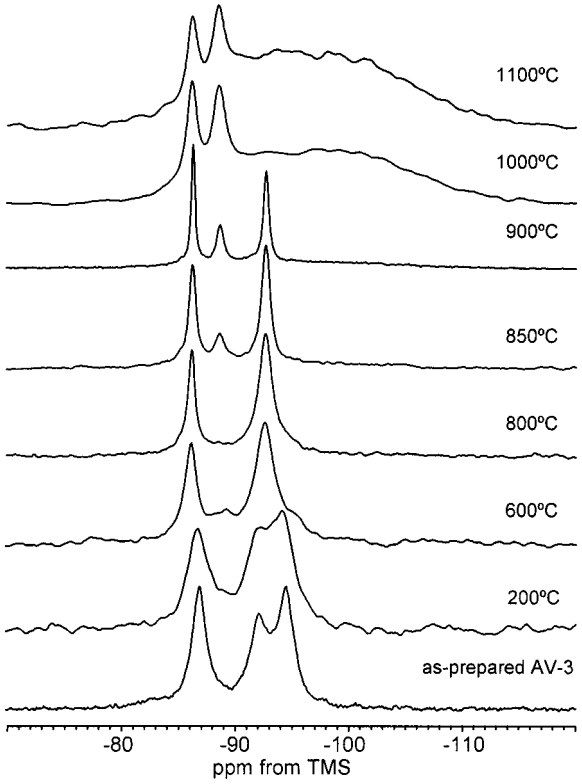

Figure 9. ^{29}Si MAS NMR spectra of AV-3 and materials calcined in air at the temperatures indicated for 6 h.

^{29}Si MAS NMR spectra of AV-3 and calcined materials are shown in Figure 9. The parent material gives three peaks at −86.6, −91.9, and −94.3 in a 1:0.9:1 intensity ratio. In accord with this observation, the crystal structure of petarasite calls for the presence of three unique Si sites with equal populations.[11] Materials dehydrated at temperatures up to 800 °C display two

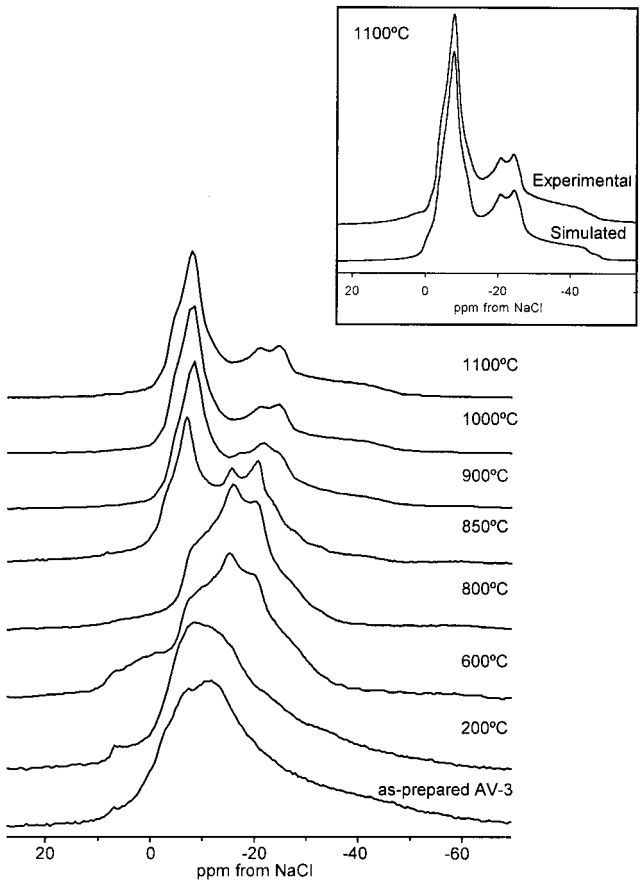

Figure 10. Single-quantum ^{23}Na MAS NMR spectra of as-prepared AV-3 and materials calcined in air at the temperatures indicated for 6 h. The inset shows a simulation of the ^{23}Na MAS NMR spectrum of AV-3 calcined at 1100 °C (synthetic parakeldyshite).

^{29}Si MAS NMR at approximately −86.2 and −92.5 ppm. Because the relative populations are in 1:2 ratios in the dehydrated material, the −91.9 and −94.3 ppm AV-3 resonances coalesce into the peak at −92.5 ppm. At 850 °C, a third peak at approximately −88.6 ppm appears, indicating the beginning of the framework collapse. This is in accord with the powder XRD evidence. Between 850 and ≈950 °C the resonance at −88.6 ppm grows while the intensity of the peak at −92.5 ppm decreases. Simultaneously, a very broad background (raised baseline) increases its intensity. Deconvolution of the 1100 °C calcined AV-3 ^{29}Si MAS NMR spectrum yields relative intensities of 0.05, 0.05, and 0.90 for the resonances at −86.0 and −88.6 ppm and the broad resonance centered at approximately −98.8 ppm, respectively. The latter corresponds to amorphous siliceous material resulting from the different stoichiometries of petarasite and parakeldyshite (the ideal Si/Zr molar ratios of petarasite and parakeldyshite are 3 and 2, respectively). For mineral parakeldyshite two different ^{29}Si MAS NMR resonances are expected with equal intensities, corresponding to two silicon sites of the type [Si(2Si,2Zr)], with equal populations. The amount of the amorphous phase present can, in principle, be quantified. The total silicon content on the calcined sample can be written as $[x(ZrSi_2) + y(ZrSi_z)]$, where x is the fraction of parakeldyshite and y is the fraction of amorphous material with the formula $ZrSi_z$ ($x + y = 1$). Because the total Si/Zr ratio in the starting material is

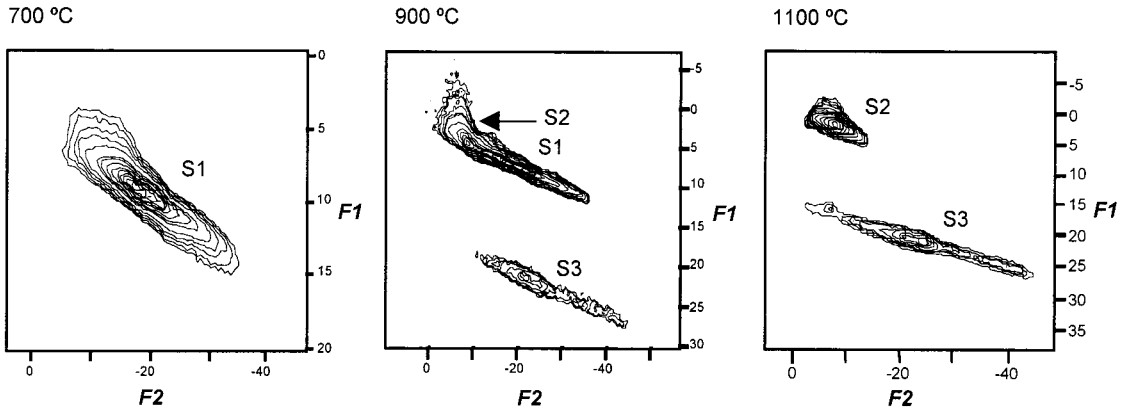

Figure 11. ^{23}Na 3Q MAS NMR spectra of AV-3 materials calcined at 700, 900, and 1100 °C (synthetic parakeldyshite).

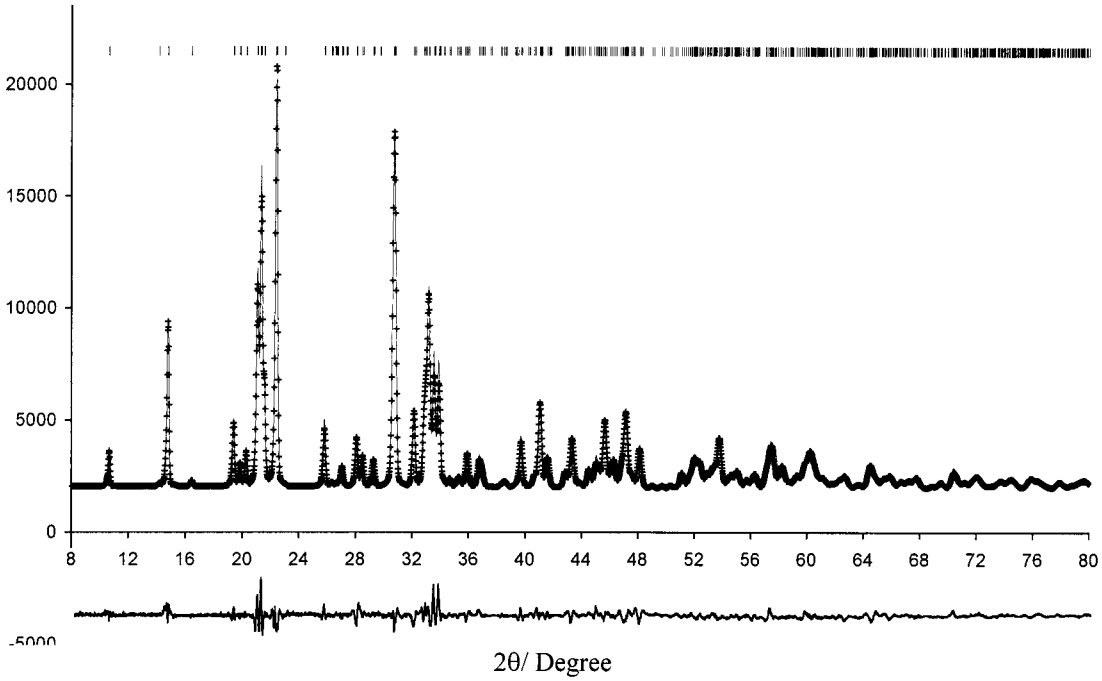

Figure 12. Observed, calculated, and difference powder XRD pattern of synthetic parakeldyshite obtained by calcining AV-3 at 1100 °C in air for 6 h.

3, [$2x + yz = 3$]. Considering the area of the ^{29}Si MAS NMR resonance corresponding to the amorphous phase is 0.90, we have (yz)/3 = 0.90. It is possible to calculate the x, y, and z values and get the total silicon content as 0.15($ZrSi_2$) + 0.85($ZrSi_{3.18}$). Eighty-five percent of the calcined material is found to be an amorphous phase with a Si/Zr ratio of 3.18 and 15% is parakeldyshite.

Single-quantum ^{23}Na MAS NMR spectra of as-prepared AV-3 and AV-3 after calcination at 200 up to 1100 °C are shown in Figure 10. AV-3 contains three crystallographically independent seven-coordinated sodium sites with equal populations, which are only resolved in the ^{23}Na 3Q MAS NMR.[10] Apparently, major changes in the ^{23}Na MAS NMR spectrum occur early (600 °C), possibly because of the dehydration of the Na(1) and Na(2) sites that have water molecules in their coordination sphere [$NaO_5(H_2O)Cl$]. ^{23}Na 3Q MAS NMR (Figure 11) and the simulation of the 700 °C single-quantum spectrum (not shown) indicate the presence of only one sodium site (S1) with an isotropic chemical shift of −5.1 ppm, quadrupole coupling constant 2.17 MHz, and asymmetry parameter 0.6. At 850 °C other resonances start to appear in the spectrum. The ^{23}Na 3Q MAS spectrum of 900 °C calcined AV-3 shows the coexistence of three different sodium sites. The single-quantum ^{23}Na MAS NMR spectrum of AV-3 calcined at 1100 °C for 15 h can be simulated (inset Figure 10), assuming the presence of two resonances (S2 and S3), as indicated on the ^{23}Na 3Q MAS spectrum (Figure 11), with intensities ≈1:0.9 and the following parameters: isotropic chemical shifts −4.1 and −2.3 ppm; quadrupole coupling constants 2.53 and 1.34 MHz; asymmetry parameters 0.81 and 0.80, respectively. In accord with this observation, the crystal structure of parakeldyshite calls for the presence of two sodium sites with equal populations.[22] It should be noticed that the ^{23}Na 3Q MAS NMR spectrum of AV-3 calcined at 900 °C shows a mixture of phases because S1, S2, and S3 are present.

Tables 1 and 5 and Figure 12 give the results of the Rietveld refinement of the structure of synthetic parakeldyshite obtained by calcining AV-3 at 1100 °C. The structure of parakeldyshite (Figure 3c) consists of layers of mixed six-membered rings formed by two double-tetrahedra Si_2O_7 linked by two isolated ZrO_6 octahedra with sodium atoms in 8-fold coordination occupying holes in the three-dimensional network. An interesting

Table 5. Atomic Coordinates and Isotropic Thermal Parameters for Synthetic Parakeldyshite (Synthetic Petarasite Calcined at 1100 °C for 15 h)

name	*x*	*y*	*z*	B_{iso} (Å^2)
Na(1)	0.878(1)	0.0930(9)	0.260(1)	2.0(2)
Na(2)	0.338(1)	0.5017(8)	0.769(1)	2.0(2)
Zr(1)	0.290(4)	0.2704(2)	0.2210(4)	1.96(6)
Si(1)	0.653(1)	0.1497(8)	0.775(1)	2.0(2)
Si(2)	0.942(1)	0.3373(7)	0.678(1)	1.3(1)
O(1)	0.296(2)	0.033(1)	0.171(2)	1.7(3)
O(2)	0.877(2)	0.172(1)	0.717(2)	1.6(3)
O(3)	0.496(2)	0.206(1)	0.540(2)	2.3(3)
O(4)	0.562(2)	0.248(1)	0.010(2)	1.0(3)
O(5)	0.004(2)	0.317(1)	0.392(2)	2.0(3)
O(6)	0.118(2)	0.324(1)	0.882(2)	1.6(3)
O(7)	0.2783(2)	0.514(1)	0.285(2)	1.5(3)

relationship exists between the structures of petarasite and parakeldyshite. The framework of petarasite (Figure 3d) is composed of corner-sharing, six-membered silicate rings linked by ZrO_6 octahedra,[11] whereas the structure of parakeldyshite is based on layers of mixed six-membered rings formed by two Si_2O_7 groups and two ZrO_6 octahedra (Figure 3c). The parakedyshite layers can be derived from the $Zr_2Si_6O_{18}$ framework of petarasite by removing the two Si(2) tetrahedra in the six-membered rings.[11] Although the refinement converged, the reliability factors were relatively poor (Table 1). This is due to the amorphous content of the calcined material. Because synthetic parakeldyshite is the product of thermal conversion of a material with higher silicon content, a large amount of amorphous siliceous material forms. This results in a powder XRD raised baseline and, as a consequence, the χ^2 refinement value is high. The bond distances (Table 3) confirm that sodium cations are octahedrally coordinated. Si(1) forms quite small Si−O bonds (average 1.580 Å) when compared with the Si(2)−O bonds (average 1.616 Å). The empirical correlation between Si−O bond lengths and the ^{29}Si NMR chemical shift[25] suggests that the resonance at −86.0 ppm is assigned to Si(2) while the resonance at −88.6 ppm is attributed to Si(1).

Conclusions

In summary, the preparation and structural characterization of synthetic analogues of the zirconosilicate minerals kostylevite (AV-8), wadeite, and parakeldyshite have been reported and the thermal transformation of AV-3 and AM-2 has been studied in detail by powder XRD, TGA, and ^{23}Na and ^{29}Si solid-state NMR.

Acknowledgment. We would like to thank FEDER and SAPIENS for financial support.

CM0007196

(25) Engelhardt, G.; Michel, D. *High-Resolution Solid-State NMR of Silicates and Zeolites*; Wiley: New York, 1987.